

Plagiasi Materials Lett Influence of ... 2020

by Marjoni Imamora Ali Umar

Submission date: 30-May-2020 09:21AM (UTC+0700)

Submission ID: 1334522743

File name: MLBLUE-D-20-01935-Accept.pdf (1.23M)

Word count: 3289

Character count: 16182

*Revised Manuscript

The Influence of MoSe₂ Coated onto Pt Film to DSSC Performance with the Structure TiO₂/Dye/L_xMoSe₂Pt (0≤x≤5)

Marjoni Imamora Ali Umar^{1*}, Resti¹, Venny Haris¹, Akrajas Ali Umar²

¹Department of Physics Education, FTIK, IAIN Batusangkar, 27213, Batusangkar, Tanah Datar, West-Sumatera, Indonesia

² IMEN, Universiti Kebangsaan Malaysia, Bangi, Selangor Darul Ehsan, Malaysia

*Correspondence: Tel: +62752-71150 Fax: +62752-71879

*Email: nurjoniimamora@yahoo.com; marjoni.imamora@iainbatusangkar.ac.id

Abstract

Research on the influence of Molybdenum Diselenide (MoSe₂) coating on platinum (Pt) to performing dye-sensitized solar cell (DSSC) with the structure of TiO₂/Dye/L_xMoSe₂Pt, (0≤x≤5) is reported. The hydrothermal method has successfully synthesized the TiO₂ film with square and porous morphology on the indium titanium oxide (ITO) surface. Four peaks of the Raman Scattering detected from the semiconductor confirm the formation of TiO₂ film. The liquid-phase deposition (LPD) also successfully prepared the Pt film. Onto the prepared Pt, the MoSe₂ was coated to produce L_xMoSe₂Pt (0≤x≤5) and then use them as the counter electrode (CE). The best DSSC devices with TiO₂/Dye/L₂MoSe₂Pt structures have resulted in current-density, Voc, and solar cell performance of 11.204 mA/cm², 0.66 V, and 2.967%, respectively. The Bode graph confirmed this device has the longest lifetime, proven by the highest peak rise in the lowest frequency. Besides, high-frequency also shows the device has low resistance, useful for accelerating the electrons flow and enhancing DSSC performance.

Keywords: Counter-electrode, semiconductors, L_xMoSe₂Pt, MoSe₂, DSSC-performance

Introduction

DSSC is a solar device with semiconductor-based which determined by the effectiveness of the photo-physiochemical phenomenon on the semiconductor [1]. As a third-generation solar-cell has several advantages, such as cheaper, simple-production, and high-efficiency [2]. We believe the efficiency might be enhanced by modifying the key components of the DSSC, such as semiconductor, CE, and electrolyte. Semiconductors which have wide band-gap energy such as TiO₂ [3] with the sense of dye-sensitized material, and the CE with high electro-catalytic, good conductivity and stable [2] could further improve the DSSC performance.

Pt is a popular CE in DSSC application due to it has high efficiency [4, 5] compared to Carbon and Graphene [6-18]. However, an effort to further enhance the Pt properties by adding or attach them to other materials has been reported. For instance, Graphene (G-Pt) and reduced graphene oxide/rGO (rGO-Pt), resulting in the efficiency increased around 0.8% and 0.9%, respectively [19]. Besides, Gong et al. added one-layer of Pt on Graphene (GNS) [6], resulting in the efficiency increased from 4.76% (Pt) to 6.09% (GNS/Pt). Besides, Cheng et al. also reported the MoS₂ addition (Pt/MoS₂) producing the device performance increase of 0.6% [20]. In this

1
2
3
4 research, we report the use of MoSe₂ as a coated layer on platinum and then used them as a CE
5 on the DSSC device. Since it has a very active electrocatalytic, good conductivity [21] and
6 resistant to corrosion caused by electrolytes [22]. The best performance obtained is 2.967% with
7 the V_{OC} and fill-factor generated by 0.66 V and 40.11%, respectively.
8
9

10 **Material and Methods**

11 *Synthesis TiO₂ and Pt + MoSe₂ (L_xMoSe₂Pt, 0 ≤ x ≤ 5)*

12
13
14
15 We purchased all chemicals in this work from Sigma-Aldrich. We synthesized TiO₂
16 semiconductor on the ITO substrate by using a growth solution which consists of 5 mL
17 Ammonium-Hexafluorotitanate and 5 mL boric acid with deionized (DI) water. The detail of the
18 synthesis process has been well-explained in the previous report [3]. Pt films were synthesized
19 using the LPD method on the ITO substrate. We started the Pt synthesis from seeding 3 times by
20 using a solution of L-Ascorbic Acid and potassium tetrachloroplatinate (K₂PtCl₄) with a
21 temperature of 50°C for 2 hours. After that, we continued to Pt growth, using a solution of
22 K₂PtCl₄, L-Ascorbic Acid, Polyvinyl pyrrolidone, and sodium hydroxide with a temperature of
23 50°C for 5 hours. Last, the prepared Pt was then annealed in an oven for 1 hour at 250°C. Next,
24 the resultant Pt was coated by MoSe₂, forming the L_xMoSe₂Pt (0 ≤ x ≤ 5) film using the LPD
25 method. The Pt film was put into the growth-solution (0.5 M of Hexamethylenetetramine 0.5 M,
26 0.05 M of Ammonium Tetrathromolybdate, 0.1 M of Sodium Borohydrate and 0.01 M of
27 Selenium) and synthesized using water-bath at 90°C for 30 minutes. We repeated these steps to
28 produce two until five layers of MoSe₂. Last, the coated Pt was annealed by hydrogen flow at
29 300°C for 3 hours. During the synthesis process, the morphology of TiO₂ and Platinum film was
30 observed with a FESEM and Raman Scattering as well.
31
32
33
34
35

36 *Preparation of DSSC Devices with the structured of TiO₂/Dye/L_xMoSe₂Pt (0 ≤ x ≤ 5)*

37
38 We designed DSSC devices as Fig. 2B to see the influence of L_xMoSe₂Pt (0 ≤ x ≤ 5) film as a
39 CE on the device performance. The TiO₂ semiconductor as a photoanode is assembled (after
40 immersed in dye solution (0.05 mM N719) at room temperature for 15 hours) with a CE using a
41 metal clamp. A para-film with a circle hole of 0.23 cm² was sandwiched between the TiO₂ and
42 the L_xMoSe₂Pt and injected the electrolyte solution. Last, the current-voltage (J-V) curve of the
43 DSSC was obtained using the Gamry instrument under illumination by simulated sunlight with
44 an intensity of 100 mW cm² to characterize the device performance.
45
46
47

48 **Results and Discussion**

49
50 FESEM image shows the synthesized TiO₂ successfully covered the entire ITO surface (see Fig.
51 1A). The TiO₂ particles have a morphology that resembles a square shape (Fig. 1B, 1C) with
52 porous structures and varying particle sizes (see Fig.1C and 1D). The porous structure is believed
53 caused by the use of high temperatures during the growth process. This condition is useful to
54 absorb more dye and enhanced DSSC performance [3]. Fig. 1E shows the Raman Scattering
55 spectrum consisting of 4 peaks of 141 cm⁻¹, 393 cm⁻¹, 513 cm⁻¹, and 636 cm⁻¹ with one peak
56 having high intensity between 100-800 cm⁻¹. The resultant peaks are comparable with the
57 research results of Tian et al. [23] and confirm the formation of TiO₂.
58
59

1
2
3
4
5
6
7 Fig. 2A is the FESEM image of Pt with asymmetrical structures (particle size of 156 ± 16 nm)
8 and covers the entire ITO surface. Next, the synthesized $L_x\text{MoSe}_2\text{Pt}$ ($0 \leq x \leq 5$) was used as CE in
9 DSSC devices with the structured $\text{TiO}_2/\text{Dye}/L_x\text{MoSe}_2\text{Pt}$ (see Fig 2B). The J-V curve of DSSC
10 and the photovoltaic parameter are described in Fig. 2C and Table 1, respectively. From the
11 Table 1 shows the DSSC performance start from 2.858%, and then decreased to 2.364% when
12 using $L_1\text{MoSe}_2\text{Pt}$ as CE. We believed, it occurred as an effect of the heating repetition during
13 MoSe_2 coating, and causing the Pt structure damaged and reduced film adhesion [24].
14 Interestingly, the DSSC performance increase when using the $L_2\text{MoSe}_2\text{Pt}$ as CE to 2.967%. In
15 this stage the MoSe_2 coating rather thick, and covering the Pt structure from directly exposed to
16 high temperature, improving the surface area and their conductivity [6]. Besides, the increasing
17 of the surface area providing sensitization of dye materials, speed-up the electrolyte redox
18 reaction [25], and producing higher performance [26]. Then, the DSSC performance decrease
19 again with the number of MoSe_2 coating layer increased ($L_3\text{MoSe}_2\text{Pt}$, $L_4\text{MoSe}_2\text{Pt}$, and
20 $L_5\text{MoSe}_2\text{Pt}$). Besides the previous reason, since the addition of each layer of MoSe_2 does not
21 followed by the annealed process, causing the bond between them still fragile and easily
22 damaged also causing this phenomenon. The best DSSC performance shows 0.11% higher than
23 the first devices and confirming the coated of MoSe_2 are successfully catalyst the Pt film [2, 27].
24 Since the TiO_2 , dye-materials [16, 18], and electrolyte-selection are far from being optimized,
25 applying the Pt in optimized device will enhanced the DSSC performance. These results also
26 support by Bode graphs (see Fig. 3) which shows that this device produces the highest peak on
27 the lowest frequency. Its means, high-frequency peaks show the device has small resistance and
28 highest lifetime compared to other [28]. Besides, the small resistance leading to speed-up the
29 flow of electrons [25], and producing the DSSC devices with the higher performance [29].

36 Conclusion

37
38 The influence of MoSe_2 coated onto Pt film to produce $L_x\text{MoSe}_2\text{Pt}$ ($0 \leq x \leq 5$) as CE on the DSSC
39 performance has been carried out. The best DSSC devices with the structure of
40 $\text{TiO}_2/\text{Dye}/L_2\text{MoSe}_2\text{Pt}$ have resulted in current density, V_{oc} , and solar cell performance of 11.204
41 mA/cm^2 , 0.66 V, and 2.967% , respectively. Bode graph confirming the device structure has the
42 highest lifetime because of the highest peak is detected on the lowest frequency. Besides, the
43 high-frequency peaks also show small device resistance, leading to accelerating the electrons
44 flow and enhanced DSSC performance.

48 Acknowledgment:

49 We would like to thank the MOHE Malaysia, Dr. H. Kasmuri, M.A. (Rector), Dr. Sirajul Munir,
50 M.Pd. (Dean), and Bundo Hj. Cherana, Fitri Yenni, M.Sc, Miftahul Farid Rafi M.I, and Cresvo
51 Fourvindra Pratama for their contribution to this work.

58 Bibliography

- 1
2
3
4
5
6 [1] A.A. Umar, S. Nafisah, S.K.M. Saad, S.T. Tan, A. Balouch, M.M. Salleh, M. Oyama,
7 Poriferous microtablet of anatase TiO₂ growth on an ITO surface for high-efficiency dye-
8 sensitized solar cells, *Sol. Energy Mater. Sol. cells* 122 (2014) 174-182.
9 [2] J. Dong, J. Wu, J. Jia, L. Hu, S. Dai, Cobalt/molybdenum ternary hybrid with hierarchical
10 architecture used as high efficient counter electrode for dye-sensitized solar cells, *Sol. Energy*
11 122 (2015) 326-333.
12 [3] A.A. Umar, S.K.M. Saad, M.I.A. Umar, M.Y.A. Rahman, M. Oyama, Advances in porous
13 and high-energy (001)-faceted anatase TiO₂ nanostructures, *Opt. Mater.* 75 (2018) 390-430.
14 [4] P. Poudel, A. Thapa, H. Elbohy, Q. Qiao, Improved performance of dye solar cells using
15 nanocarbon as support for platinum nanoparticles in counter electrode, *Nano Energy* 5 (2014)
16 116-121.
17 [5] A. Iefanova, J. Nepal, P. Poudel, D. Davoux, U. Gautam, V. Mallam, Q. Qiao, B. Logue,
18 M.F. Baroughi, Transparent platinum counter electrode for efficient semi-transparent dye-
19 sensitized solar cells, *Thin Solid Films* 562 (2014) 578-584.
20 [6] F. Gong, H. Wang, Z.-S. Wang, Self-assembled monolayer of graphene/Pt as counter
21 electrode for efficient dye-sensitized solar cell, *Phys.Chem. Chem. Phys.* 13(39) (2011) 17676-
22 17682.
23 [7] M.I. Ali Umar, C.C. Yap, R. Awang, A. Ali Umar, M. Mat Salleh, M. Yahaya, Formation of
24 gold-coated multilayer graphene via thermal reduction, *Mater Lett* 106 (2013) 200-203.
25 [8] L.-L. Li, C.-W. Chang, H.-H. Wu, J.-W. Shiu, P.-T. Wu, E.W.-G. Diao, Morphological
26 control of platinum nanostructures for highly efficient dye-sensitized solar cells, *J. Mater. Chem.*
27 22(13) (2012) 6267-6273.
28 [9] J. Gong, Z. Zhou, K. Sumathy, H. Yang, Q. Qiao, Activated graphene nanoplatelets as a
29 counter electrode for dye-sensitized solar cells, *J. Appl. Phys* 119(13) (2016) 135501.
30 [10] A. Aboagye, H. Elbohy, A.D. Kelkar, Q. Qiao, J. Zai, X. Qian, L. Zhang, Electrospun
31 carbon nanofibers with surface-attached platinum nanoparticles as cost-effective and efficient
32 counter electrode for dye-sensitized solar cells, *Nano Energy* 11 (2015) 550-556.
33 [11] P. Poudel, Q. Qiao, Carbon nanostructure counter electrodes for low cost and stable dye-
34 sensitized solar cells, *Nano Energy* 4 (2014) 157-175.
35 [12] Z. Zhou, S. Sigdel, J. Gong, B. Vaagensmith, H. Elbohy, H. Yang, S. Krishnan, X.-F. Wu,
36 Q. Qiao, Graphene-beaded carbon nanofibers with incorporated Ni nanoparticles as efficient
37 counter-electrode for dye-sensitized solar cells, *Nano Energy* 22 (2016) 558-563.
38 [13] P. Poudel, L. Zhang, P. Joshi, S. Venkatesan, H. Fong, Q. Qiao, Enhanced performance in
39 dye-sensitized solar cells via carbon nanofibers-platinum composite counter electrodes,
40 *Nanoscale* 4(15) (2012) 4726-4730.
41 [14] Y. Zhao, A. Thapa, Q. Feng, M. Xi, Q. Qiao, H. Fong, Electrospun TiC/C nano-felt surface-
42 decorated with Pt nanoparticles as highly efficient and cost-effective counter electrode for dye-
43 sensitized solar cells, *Nanoscale* 5(23) (2013) 11742-11747.
44 [15] X. Ma, H. Elbohy, S. Sigdel, C. Lai, Q. Qiao, H. Fong, Electrospun carbon nano-felt derived
45 from alkali lignin for cost-effective counter electrodes of dye-sensitized solar cells, *RSC*
46 *advances* 6(14) (2016) 11481-11487.
47 [16] Q. He, S. Huang, J. Zai, N. Tang, B. Li, Q. Qiao, X. Qian, Efficient counter electrode
48 manufactured from Ag₂S nanocrystal ink for dye- sensitized solar cells, *Chemistry-A European*
49 *Journal* 21(43) (2015) 15153-15157.
50
51
52
53
54
55
56
57
58

- 1
2
3
4
5
6 [17] Q. He, S. Huang, C. Wang, Q. Qiao, N. Liang, M. Xu, W. Chen, J. Zai, X. Qian, The Role
7 of Mott–Schottky Heterojunctions in Ag–Ag₈SnS₆ as Counter Electrodes in Dye- Sensitized
8 Solar Cells, *ChemSusChem* 8(5) (2015) 817-820.
9 [18] Q. He, T. Qian, J. Zai, Q. Qiao, S. Huang, Y. Li, M. Wang, Efficient Ag₈GeS₆ counter
10 electrode prepared from nanocrystal ink for dye-sensitized solar cells, *J. Mater. Chem. A* 3(40)
11 (2015) 20359-20365.
12 [19] R. Bajpai, S. Roy, P. Kumar, P. Bajpai, N. Kulshrestha, J. Rafiee, N. Koratkar, D. Misra,
13 Graphene supported platinum nanoparticle counter-electrode for enhanced performance of dye-
14 sensitized solar cells, *ACS Appl. Mater. interfaces* 3(10) (2011) 3884-3889.
15 [20] C.-K. Cheng, J.-Y. Lin, K.-C. Huang, T.-K. Yeh, C.-K. Hsieh, Enhanced efficiency of dye-
16 sensitized solar counter electrodes consisting of two-dimensional nanostructural molybdenum
17 disulfide nanosheets supported Pt nanoparticles, *Coat.* 7(10) (2017) 167.
18 [21] Y. Huang, H. Lu, H. Gu, J. Fu, S. Mo, C. Wei, Y.-E. Miao, T. Liu, A CNT@ MoSe₂ hybrid
19 catalyst for efficient and stable hydrogen evolution, *Nanoscale* 7(44) (2015) 18595-18602.
20 [22] N. Jena, A. De Sarkar, Compressive strain induced enhancement in thermoelectric-power-
21 factor in monolayer MoS₂ nanosheet, *J. Phys. Condens. Matter* 29(22) (2017) 225501.
22 [23] F. Tian, Y. Zhang, J. Zhang, C. Pan, Raman spectroscopy: a new approach to measure the
23 percentage of anatase TiO₂ exposed (001) facets, *J. Phys. Chem. C* 116(13) (2012) 7515-7519.
24 [24] Y.L.F. Musico, C.M. Santos, M.L.P. Dalida, D.F. Rodrigues, Improved removal of lead (II)
25 from water using a polymer-based graphene oxide nanocomposite, *J. Mater. Chem. A* 1(11)
26 (2013) 3789-3796.
27 [25] G. Yue, J. Wu, Y. Xiao, M. Huang, J. Lin, J.-Y. Lin, High performance platinum-free
28 counter electrode of molybdenum sulfide–carbon used in dye-sensitized solar cells, *J. Mater.*
29 *Chem. A* 1(4) (2013) 1495-1501.
30 [26] M.I.A. Umar, F.Y. Naumar, M.M. Salleh, A.A. Umar, Hydrothermally grown of well-
31 aligned ZnONRs: dependence of alignment ordering upon precursor concentration, *J. Mater. Sci-*
32 *Mater. El.* 29(8) (2018) 6892-6897.
33 [27] A. Abderrahmane, P. Ko, T. Thu, S. Ishizawa, T. Takamura, A. Sandhu, High
34 photosensitivity few-layered MoSe₂ back-gated field-effect phototransistors, *Nanotechnology*
35 25(36) (2014) 365202.
36 [28] A. Lim, N. Haji Manaf, K. Tennakoon, R. Chandrakanthi, L.B.L. Lim, J. Bandara, P.
37 Ekanayake, Higher performance of DSSC with dyes from *Cladophora* sp. as mixed cosensitizer
38 through synergistic effect, *J. Biophys.* 2015 (2015).
39 [29] T. Sawatsuk, A. Chindaduang, C. Sae-Kung, S. Pratontep, G. Tumcharern, Dye-sensitized
40 solar cells based on TiO₂–MWCNTs composite electrodes: Performance improvement and their
41 mechanisms, *Diamond Relat. Mater.* 18(2-3) (2009) 524-527.
42
43
44
45
46
47
48

1
2
3
4
5
6
7
8
9
10
11
12
13
14
15
16
17
18
19
20
21
22
23
24
25
26
27
28
29
30
31
32
33
34
35
36
37
38
39
40
41
42
43
44
45
46
47
48

49
50
51
52
53
54
55
56
57
58
59
60
61
62
63
64
65

Figure Captions

Fig. 1. **A-D)** are the FESEM image of a TiO₂ semiconductor film, and **E)** The Raman Scatering Spectra of TiO₂

Fig. 2. **A).** The FESEM image of Pt film (magnification of 50,000 times), **B).** DSSC array with the MoSe₂ coating. **C).** The J-V curve of DSSC devices with the structure TiO₂/Dye/L_xMoSe₂Pt (0≤x≤5).

Table 1 The photovoltaic parameters of DSSC device with the structure TiO₂/Dye/L_xMoSe₂Pt (0≤x≤5)

Fig. 3 Bode graphics of 6 DSSC devices with structure TiO₂/Dye/L_xMoSe₂Pt (0≤x≤5)

Figure and Table

The Influence of MoSe₂ Coated onto Pt Film to DSSC Performance with the Structure TiO₂/Dye/L_xMoSe₂Pt (0 ≤ x ≤ 5)

Marjoni Imamora Ali Umar^{1*}, Resti¹, Venny Haris¹, Akrajas Ali Umar²

¹Department of Physics Education, FTIK, IAIN Batusangkar, 27213, Batusangkar, Tanah Datar, West-Sumatera, Indonesia

² IMEN, [Universiti Kebangsaan Malaysia, Bangi, Selangor Darul Ehsan, Malaysia](#)

Correspondence: Tel: +62752-71150 Fax: +62752-71879

*Email: nurjoniimamora@yahoo.com; marjoni.imamora@iainbatusangkar.ac.id

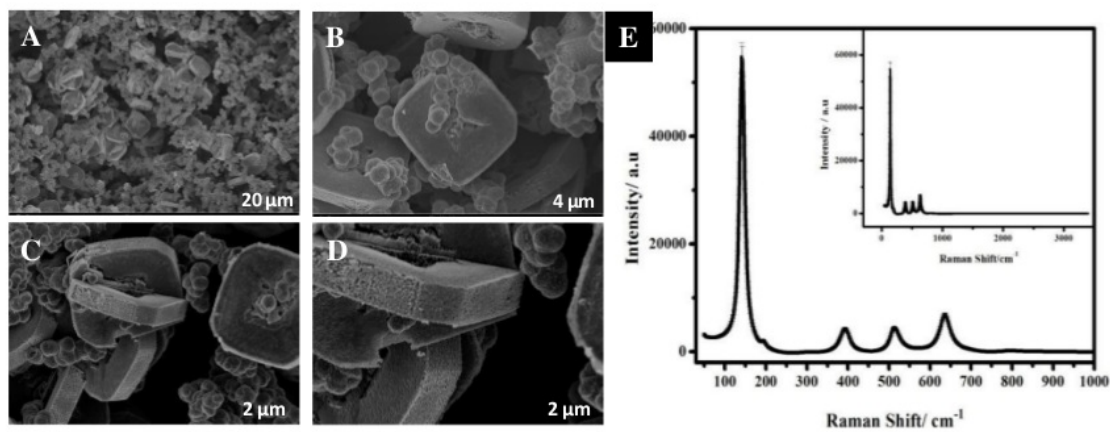


Fig. 1

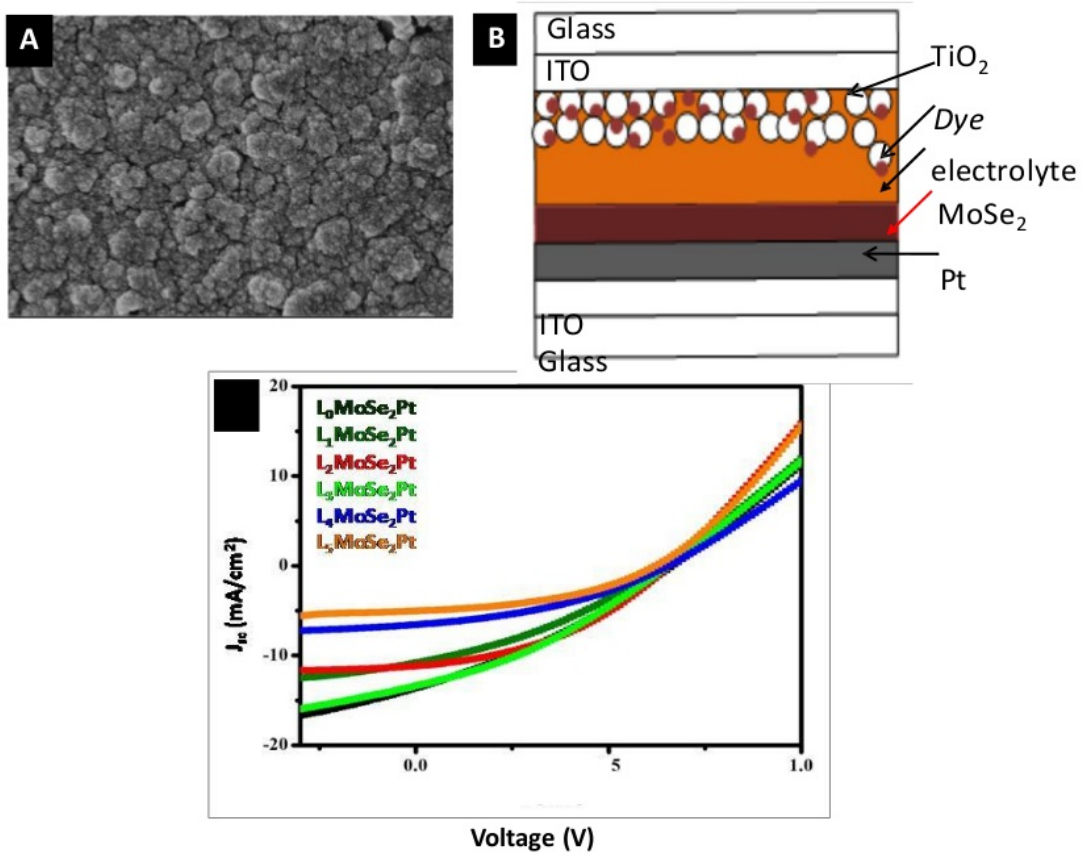


Fig. 2

Tabel 10

CE	Voc (V)	Jsc (mA/cm ²)	FF(%)	Eff (%)
L ₀ MoSe ₂ Pt	0.67	13.635	31.26	2.858
L ₁ MoSe ₂ Pt	0.65	10.861	33.47	2.364
L ₂ MoSe ₂ Pt	0.66	11.204	40.11	2.967
L ₃ MoSe ₂ Pt	0.66	13.426	32.92	2.921
L ₄ MoSe ₂ Pt	0.66	6.600	37.67	1.644
L ₅ MoSe ₂ Pt	0.63	5.078	42.13	1.350

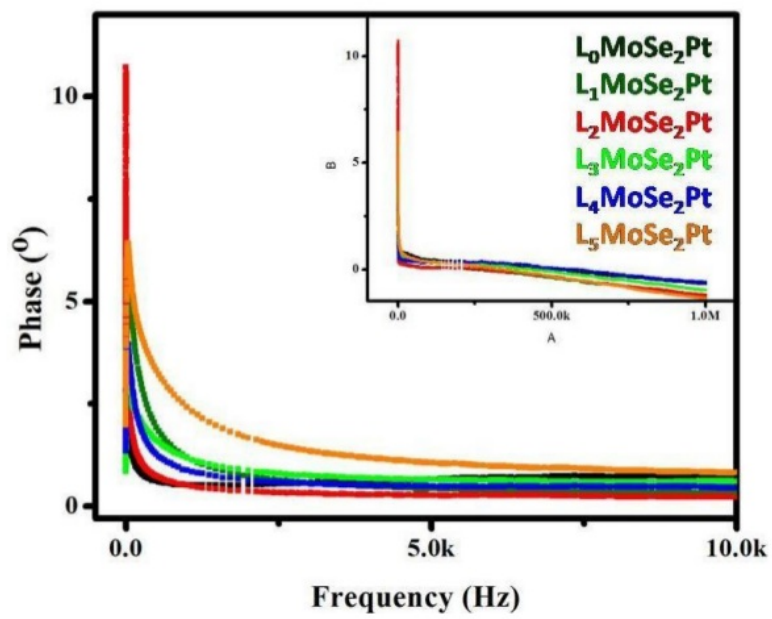


Fig 3

Credit Author Statement

The Influence of MoSe₂ Coated onto Pt Film to DSSC Performance with the Structure TiO₂/Dye/L_xMoSe₂Pt (0≤x≤5)

Marjoni Imamora Ali Umar^{1*}, Resti¹, Venny Haris¹, Akrajas Ali Umar²

¹Department of Physics Education, FTIK, IAIN Batusangkar, 27213, Batusangkar, Tanah Datar, West-Sumatera, Indonesia

²IMEN, Universiti Kebangsaan Malaysia, Bangi, Selangor Darul Ehsan, Malaysia

*Email: nurjoniimamora@yahoo.com; marjoni.imamora@iainbatusangkar.ac.id

Marjoni Imamora Ali Umar: Data Analysis, Conceptualization, Methodology, Writing-Original draft preparation, Reviewing and Editing.

Resti.: Investigation, Data Collection, Writing- draft preparation.

Venny Haris: Investigation and Validation.

Akrajas Ali Umar: Supervision, Conceptualization, Methodology Reviewing and Editing.

14 Declaration of Interest Statement

Declaration of interests

The authors declare that they have no known competing financial interests or personal relationships that could have appeared to influence the work reported in this paper.

The authors declare the following financial interests/personal relationships which may be considered as potential competing interests:

*Conflict of Interest

[Click here to download Conflict of Interest: comflict of interest 2k.docx](#)

Plagiasi Materials Lett Influence of ... 2020

ORIGINALITY REPORT

6%

SIMILARITY INDEX

4%

INTERNET SOURCES

6%

PUBLICATIONS

%

STUDENT PAPERS

PRIMARY SOURCES

1	www.intechopen.com Internet Source	1%
2	Muhamad Adam Ramli, Siti Khatijah Md Saad, Elvy Rahmi Mawarnis, Marjoni Imamora Ali Umar et al. "Facile charge transfer in fibrous PdPt bimetallic nanocube counter electrodes", <i>New Journal of Chemistry</i> , 2019 Publication	1%
3	nanoscalereslett.springeropen.com Internet Source	1%
4	N. Soin, B.Y. Majlis. "Realization of perfect silicon corrugated diaphragm using KOH etching", 2004 IEEE International Conference on Semiconductor Electronics, 2004 Publication	<1%
5	www.mdpi.com Internet Source	<1%
6	Marjoni Imamora Ali Umar, Chi Chin Yap, Rozidawati Awang, Mohammad Hafizuddin Hj Jumali, Muhamad Mat Salleh, Muhammad	<1%

Yahaya. "Characterization of multilayer graphene prepared from short-time processed graphite oxide flake", Journal of Materials Science: Materials in Electronics, 2012

Publication

7

www.titanshield.com

Internet Source

<1%

8

Li, Wenhui, Liping Si, Zonghao Liu, Zhixin Zhao, Hongshan He, Kai Zhu, Brian Moore, and Yi-Bing Cheng. "Fluorene functionalized porphyrins as broadband absorbers for TiO₂ nanocrystalline solar cells", Journal of Materials Chemistry A, 2014.

Publication

<1%

9

Sin Tee Tan, Akrajas Ali Umar, Muhamad Mat Salleh. "(001)-Faceted hexagonal ZnO nanoplate thin film synthesis and the heterogeneous catalytic reduction of 4-nitrophenol characterization", Journal of Alloys and Compounds, 2015

Publication

<1%

10

Ling Li, Huidong Sui, Kaifeng Zhao, Wenming Zhang, Xiaowei Li, Shuang Liu, Kun Yang, Mingxing Wu, Yucang Zhang. "Preparation of carbon nanofibers supported MoO₂ composites electrode materials for application in dye-sensitized solar cells", Electrochimica Acta,

<1%

2018

Publication

11

Jiawei Gong, Zhengping Zhou, K. Sumathy, Huojun Yang, Qiquan Qiao. "Activated graphene nanoplatelets as a counter electrode for dye-sensitized solar cells", Journal of Applied Physics, 2016

Publication

<1%

12

Zahra Zolfaghari-Isavandi, Zahra Shariatinia. "Fabrication of CdS quantum dot sensitized solar cells using nitrogen functionalized CNTs/TiO₂ nanocomposites", Diamond and Related Materials, 2018

Publication

<1%

13

worldwidescience.org

Internet Source

<1%

14

authors.library.caltech.edu

Internet Source

<1%

Exclude quotes On

Exclude matches Off

Exclude bibliography On